Handling of Polymer Particles in Microchannels

Alain Marcati, Christophe A. Serra, Michael Bouquey, Laurent Prat

Alain Marcati[1]
Christophe Serra[2]
Michael Bouquey[2]
Laurent Prat[1]

[1] Institut National Polytechnique de Toulouse, Université de Toulouse, Laboratoire de Génie Chimique, Toulouse, France.

[2] Ecole Européenne de Chimie, Polymères et Matériaux de Strasbourg, Laboratoire d'Ingénierie des Polymères pour les Hautes Technologies, Strasbourg, France.

Research Article

Handling of Polymer Particles in Microchannels

This paper deals with solid-liquid operations in microchannels. Continuous operations on solids (modification of frequency, change of solvent, encapsulation) in order to handle polymer particles in microchannels are described in terms of the limits of operating conditions and their possible applications. A methodology to design and implement operations on polymer particles is presented here. It is applied for the generation of onion-like structures. A microdevice completely built with Plexiglas plates and fused silica capillaries is used. The device includes droplet generation, polymerization and microparticle flow manipulation. The particles manipulated are in the range of 70 to 200 microns with a very low index of polydispersity.

Keywords: Design principles, Microcapsules, Microreactors, Polymerization

1 Introduction

Microreactors are receiving growing interest in polymerization processes [1, 2]. The micron-sized dimension is directly used for precise size distribution of the solid obtained [3, 4]. The use of microfluidics allows the attainment of polymeric particles with different shapes and compositions. Directly derived from the shape of the droplets, polymer beads [5–7], disks, and plugs [7, 8] were thus synthesized. Moreover, microfluidics enables the formation of multiphase droplets [9] from which partial polymer spheres [10], Janus [11], and ternary polymer particles [12] were obtained. In each case, synthesized polymeric particles have an extreme regularity and a broad range of size is available.

An important issue is now to be able to implement operations in continuous on the generated microparticles. This will allow the construction of more complex structures (onion-structured microparticles, assemblies of particles, etc.). From a process engineering point of view, multiple operations and their couplings are then needed (multiple operation connection, addition of a secondary fluid, solvent change or increase, or the decrease of interval length between two particles). This study is focused on a methodology to analyze a complex multi-operation system to produce a specific micro-object. From the analysis, a technological solution is proposed and validated in terms of operations performed and coupling feasibility. Three main operations are considered: droplet generation, reaction, and successive encapsulation.

2 System Analysis

In order to create onion-like structures, a clear sequence to apply to the particle flow has first to be developed. Preliminary analysis of the system is proposed in order to define which steps are necessary and what could be the technological responses to meet the objectives.

With a hypothesis on the shape factor of the droplet, a geometric pattern (Fig. 1) of a droplet chain moving in a continuous flow can be described by four measurable variables: drop length (L_g [1)]), width (w_g), velocity (v), and frequency of generation (f); the characterization of flow is reduced to three variables in the case of spherical droplets. From these data, it is possible to calculate the other dimensions: length of the pattern ($L_{pattern}$), length of the interval between droplets (L_i), volumes, etc. In addition, the two immiscible phases are charac-

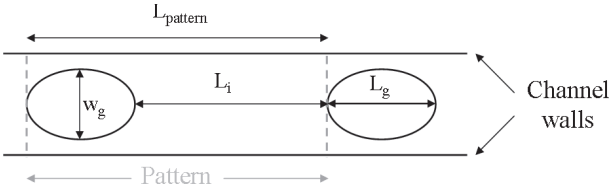

Figure 1. Droplet pattern inside the microchannels.

Correspondence: Dr. L. Prat (Laurent.Prat@ensiacet.fr), Institut National Polytechnique de Toulouse, Université de Toulouse, Laboratoire de Génie Chimique, UMR CNRS 5503, Toulouse, France.

1) List of symbols at the end of the paper.

terized with their physico-chemical properties ($\varphi\chi$): viscosity, density, and surface tension between the two phases.

The whole microsystem can thus be characterized with this geometric pattern (Fig. 2). Each block has entry variables, outlet variables, action parameters, and discrete parameters.

The generation block forms the droplet pattern; the flow rates of the continuous phase, Q_c, and dispersed phase, Q_d, are directly responsible of the variables of the pattern. The geometry of the reactor, for instance, T or cross-junction and the material of the channel, especially its roughness (R_c) or the contact angle with the fluid (θ), also have an impact on the pattern, but this impact is much more difficult to quantify.

The reaction block transforms the droplet pattern into a particle pattern depending on the length (l_p), width (w_p), velocity, and frequency of the particle. The length, L, and the diameter, d, of the channel influence the exposition time of droplets flowing at a velocity, v. Energy brought by temperature ($T°$) or UV light ($h\upsilon$) in our case creates the particles.

The encapsulation of the particles needs the injection of a new phase at a flow rate, Q_3. The third phase makes the pattern more complicated to characterize. New variables appear, such as the number of particles included (N_{int}), the length (L_{ext}), the width (w_{ext}), the velocity (v_{ext}), and the frequency (f_{ext}) of the generation of the external droplet. In this case again, the roughness and the geometry of the encapsulation area have discrete parameters.

These three blocks can be directly connected to each other, but a transfer block can also be added between them in order to change the frequency of the droplet, or particles flow, or change the solvent around the dispersion. It can be composed of a single or some secondary channels having an angle, a, with the main channel. This block is the most complex, because it has to deal with the compatibility between the phases added or withdrawn, or the compatibility between the fluids and the material. It will then define some of the limits of the operation conditions for each intervention on the flow, such as the flow rate of injection or aspiration and the global geometry of the block.

Thanks to these transfer blocks, the manipulation of the flow and the selection of phases involved in the multiple-layer structure are possible. After the encapsulation block, a new reaction block can be connected in order to create a new solid layer and then encapsulate again. Each new layer added makes the geometrical pattern more complex to describe and an increasing number of variables will be necessary to describe it.

3 Experimental Material

3.1 Multi-Block Microsystem

The microparticle management unit system (Fig. 3) is divided into three parts, providing three different process operations: droplet generation, the polymerization part, and the microparticle management unit. A detailed description of device manufacturing is presented in a previous article [13] but, in this article, chloroform – which has the property to dissolve Plexiglas – is used to seal the devices.

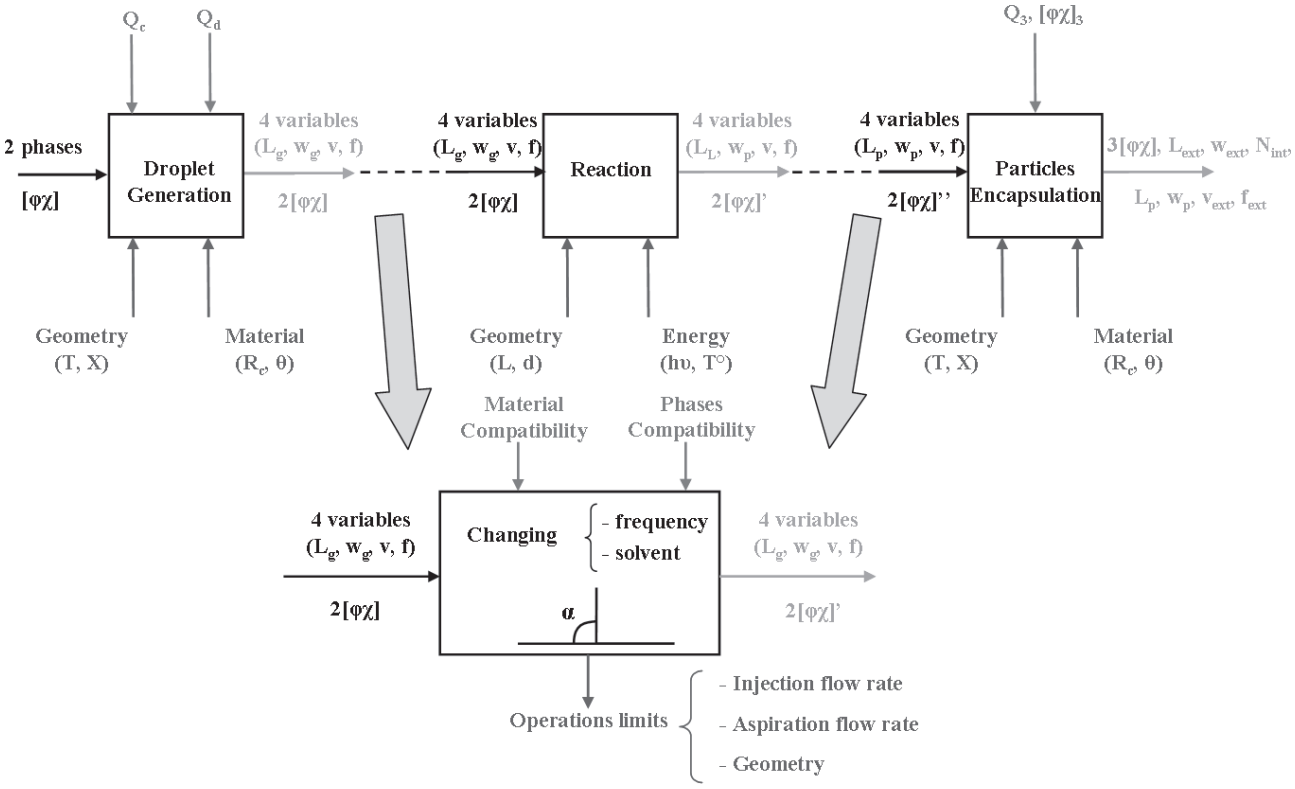

Figure 2. Characterization of the whole microsystem using the droplet pattern.

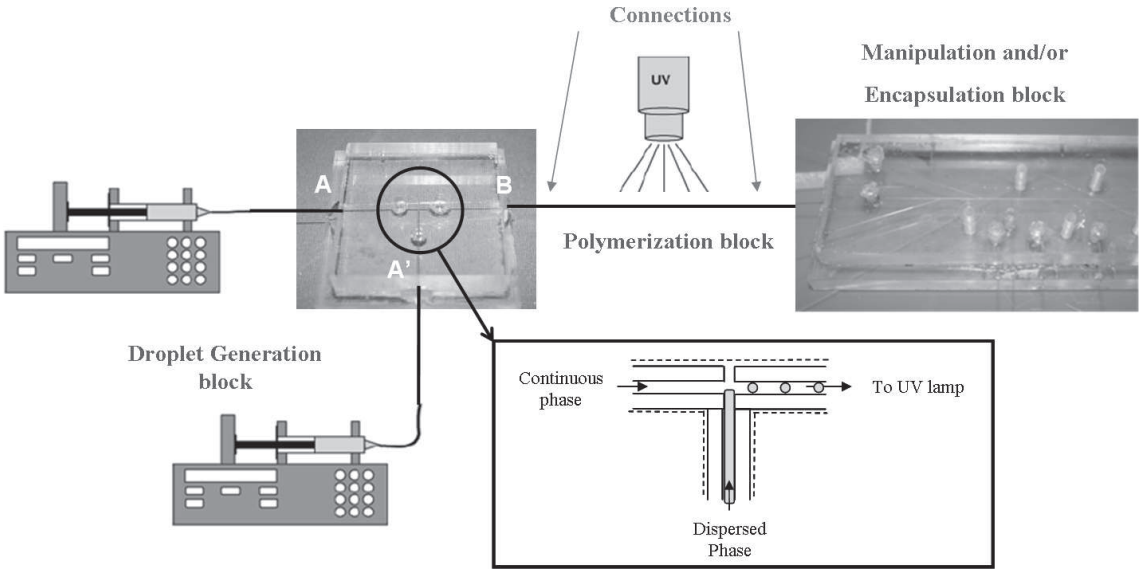

Figure 3. Schematic representation of the complete microparticle management unit system.

3.1.1 Droplet Generation Unit

The droplet generation unit can either be a T or a cross-junction. It is composed of two Plexiglas plates and standard 360-micron outer diameter (OD) capillaries; different inner diameters (ID) can be used. The first plate is worked with a micro-milling machine and a 300-micron drill. The channels thus created host the capillaries that are put in contact all together at the T-junction and fixed with glue when correctly set. The second plate is then sealed thereupon to close the generator thanks to chloroform. Capillaries of 180-micron inner diameters are used in this study.

3.1.2 Connections and Polymerization Block

The polymerization unit is composed of a single capillary whose length can vary to ensure good exposure time to UV light. Standard 360-µm capillaries made of fused silica have 20 microns-thick polyimide coating. This coating is useful to protect against capillary breaking, but absorbs UV light which prohibits polymerization, so it has to be removed. The connection between the different units is possible due to larger capillaries (320-µm ID, 465-µm OD). Polyimide coating is to be removed from 360-µm capillaries in order to be inserted into the larger ones. Capillaries from both units are set in straight contact and glued. No leakage is observed and there is neither droplet deformation nor clogging due to polymer particles.

3.1.3 Microparticle Management Unit

The last part of the microfluidic system is derived from previous studies on secondary channels [14], which have shown that it is possible to act on the continuous phase without disturbance on the dispersed phase. The secondary channels will either extract continuous phase or inject a second fluid. Fluid extraction has to face the respective pressure drop within the main or secondary channels. A right balance is to be found for effective aspiration.

As for the droplet generator, two Plexiglas plates and standard 360-µm OD capillaries are used to produce this unit. The first plate is milled with 300-µm drills according to a predefined computer-aided design. When all the capillaries are in place, the second plate is added and both plates are sealed with chloroform injected into secondary channels. All the channels have a square section of $380 \times 380\,\mu m$ so that they can host 360-µm capillaries. The angles between the main and secondary channels have been fixed to 90° or 20°. This last value is the minimum possible to ensure a good design during the milling process.

3.2 Chemical System and Solutions

Tripropylen-glycol diacrylate is used as the organic phase liquid. An initiator of photo-induced polymerization (hydroxyl-cyclohexyl-phenyl ketone) is added to the monomer to produce a 5.0-wt % mixture [5]. This chemical system is described in previous studies on polymerization in microchannels. It has the advantage to be very reactive thanks to two acrylate groups and, thus, interesting to produce microparticles with short exposition time.

An aqueous solution of bromothymol blue (BTB) is used during the manufacturing process in order to protect the main channels during the injection of chloroform. 1,4-Butanediol is used as a test fluid for the change of continuous phase around particles and 1-octanol is used as a test fluid for the encapsulation of particles.

3.3 Surrounding Equipment

The fluids are stocked into 1 to 20-mL syringes (Terumo, BD) placed on syringe pumps (Harvard 2000, Picoplus). The connection with the capillaries is made with a 22G needle (Terumo) directly glued onto them with cyanolithe glue. The observation is made with a fast CCD camera (NV1000) coupled with a microscope (Nikon SMZ-10). The image acquisition rate is 900 frames per second. Exposition time is chosen in order to have enough light for contrast distinction and short exposition for the droplet edge sharpness. A 100-W spot lamp is used to provide the necessary light. The images are acquired with transmission light through Plexiglas.

4 Results and Discussion

In the first part, the generation and the polymerization of droplets inside capillaries are described. Then, a microparticle management unit is connected to the reaction part in order to perform operations on the particle flow. The complete device (connections and sealing) is resistant up to 30 mL h^{-1}, which can be evaluated as a 0.2 bar m^{-1} pressure drop. In the experimental domain studied, no leakage is observed but sensible points concern the glue which ensures the sealing between the capillaries and Plexiglas channels.

4.1 Monomer Droplet Generation and Polymerization

Before polymerizing the droplets, several experiments were performed in order to find an operating domain where droplets and, consequently, particles have a spherical shape. The generation of the monomer droplets at a cross-junction is described by Fig. 4. The dispersed phase is injected from the capillary on the left and is maintained between the two inlets of the continuous phase. The generation of the droplet is obtained in the outlet capillaries; a thin film enters the capillary and starts to develop until it forms a droplet while advancing in the tube. When the drop is fully created, it is released and the film of dispersed phase goes back to the entrance of the outlet capillary.

The size of the droplets follows the same correlation observed for silicon oil in water in a previous article [13]. The operating domain is now set: the dispersed phase varies from 20 to 500 µL h^{-1} and the continuous phase from 4000 to 10 000 µL h^{-1}. Due to the very low thickness of the fluid in the capillary submitted to the UV lamp, the residence time necessary to obtain solid particles is reduces down to about 5 s or even less. Fig. 5 shows the particle size distribution through the operating conditions.

Monodisperse particles of different size and shape are obtained in the range of 70 to 200 microns. Classically, particle size decreases with the increase in continuous phase flow rate and increases when the dispersed phase is raised. Particle shape varies with monomer flow rate; a hydrodynamic break on the dimension of the particles is observed for each continuous flow rate. As water flow rate increases, the break happens for higher monomer flow rate. It is marked in Fig. 5, and corresponds to the limit between polymer beads and bullet-shaped particles. At low monomer flow rate (inferior to 200 µL h^{-1}), particles are thus spherical and no satellite particles are observed; when they are recovered on a glass sheet, they automatically set themselves in regular hexagonal structures. The coefficient of variation in the particle diameter is measured on over 150 particles by image analysis. For all the spherical particles, it is located between 0.8 and 1.5 %. An example is given on the upper graph of Fig. 5. At higher monomer flow rates, particles assume this bullet shape, and satellites become as numerous and visible as the flow rate is high.

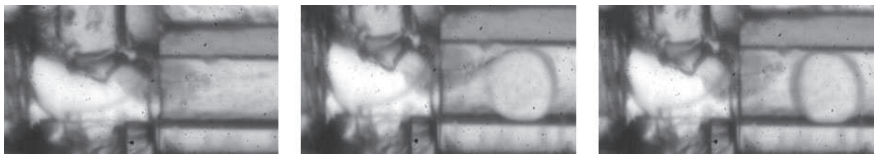

Figure 4. Generation of monomer droplets at a cross-junction inside capillaries: water flow rate at 10 mL h^{-1}; monomer flow rate at 0.2 mL h^{-1}.

4.2 Continuous Phase Aspiration

The frequency of particles flowing inside the microchannel is originally determined by the ratio of the continuous and dispersed flow rates. It can easily be regulated by withdrawing or adding continuous phase. Particle velocity is then reduced or accelerated. In order to select the best configuration and operating conditions to change the continuous phase around the particles, a comparison between a Y junction with an angle of 20° and a T-junction is made. Even if the particles are not perfectly spherical, these experiments are lead with a dense medium of particles (water flow rate of 4 mL h^{-1}; monomer flow rate of 100 µL h^{-1}). The flows with particles widely spaced seem indeed simpler to manipulate than particles flowing very close to each other. As particles may clog the secondary channel if they are brought in by the aspiration, it is important to find the limit in the flow rates of aspiration applied. Consequently, a comparison between a particle flow and a droplet flow is first made.

4.2.1 Aspiration with Droplets and Particles

The images taken during the manipulation of the flow are presented in Fig. 6. With particle flow, the withdrawal flow rate is cautiously increased. The distance between particles decreases progressively until they touch each other at 2 mL h^{-1}, but this state is unstable and particles begin to put themselves in staggered rows. At 2.5 mL h^{-1}, particles move into the withdrawal channel. The aspiration flow should then be lower than 2 mL h^{-1}.

With droplet flow, the aspiration flow rate is increased until all the droplets are drained into the secondary

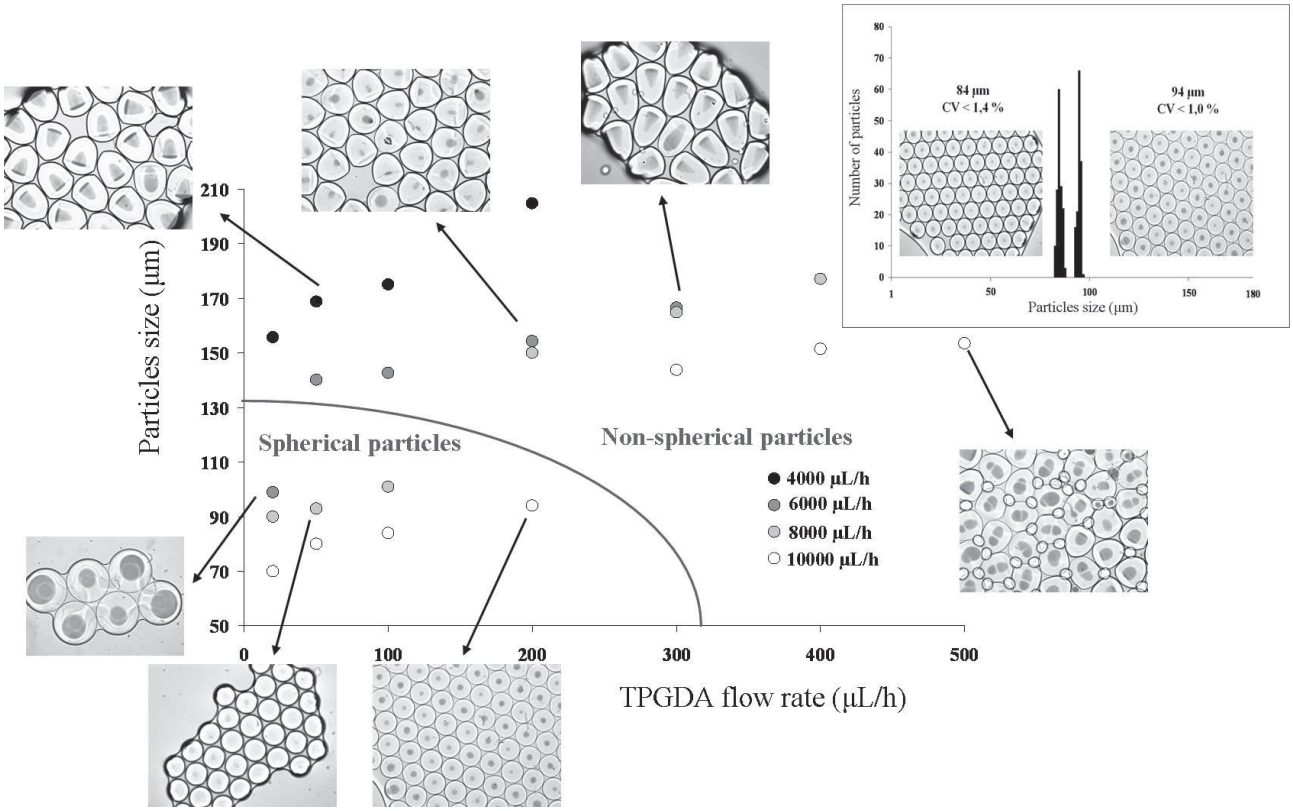

Figure 5. Cartography of particles obtained in a cross-junction and measurement of the variation coefficient for the particle diameter (upper graph).

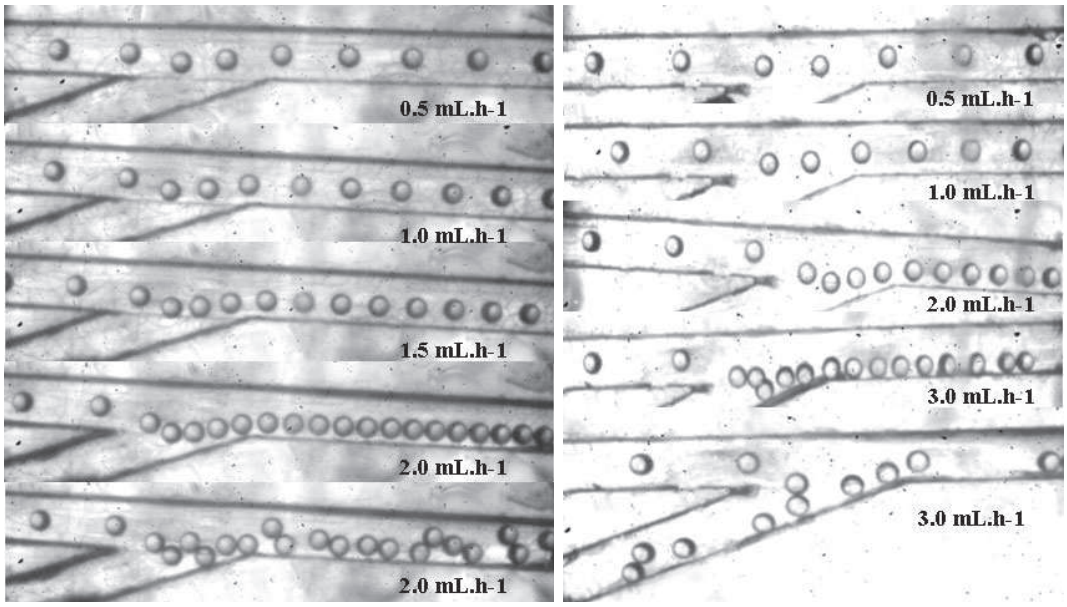

Figure 6. Progressive aspiration of the continuous phase in a particle flow (left) and a droplet flow (right).

channel. The distance between droplets and walls slowly decreases until some may explode with the shock. At 3 mL h^{-1}, flow starts to be chaotic and droplets can switch to the secondary channel. At 4 mL h^{-1}, droplets move into the secondary channel after a few seconds. Then flow is regular in the withdrawal channel and droplets do not touch the walls. An aspiration flow rate of 2.5 mL h^{-1} is then a limit to prevent droplets from directing into the secondary channel.

There is a little difference in the maximum flow rate of aspiration, but the behavior of droplets and particles during continuous phase aspiration is similar. It is simpler then to study the withdrawal of the continuous phase with droplets because, even if they explode by contact with the walls, they can be cleaned, whereas particles may totally clog the channels and consequently the microsystem.

4.2.2 Determination of the Angle of the Aspiration Channel

The withdrawal of continuous phase around droplets is then tested in a T-junction with the same operating conditions (Fig. 7). The aspiration flow rate is progressively increased until droplets are drained into the secondary channel. At 1.5 mL h^{-1}, the droplets are very close to the angle of the secondary channels. When the aspiration flow rate is at 2 mL h^{-1}, some droplets may explode at the angle and some droplets are attracted into the secondary channel.

Fig. 7 compares the aspiration efficiency with an angle of 20° and an angle of 90° function of the aspiration flow rate. The aspiration efficiency is defined as the difference between distance without aspiration (initial interval between droplets) and the distance with aspiration, divided by the initial interval between droplets. At low aspiration flow rate, the response is pretty similar for each angle but, when aspiration is further increased, there is a strong disparity between the two angles. Not only the angle of 20° allows recovering more continuous phase, but the limit of aspiration is even higher than that of the T-junction. The angle of 20° seems thus much more interesting for the withdrawal of the continuous phase. This difference can be explained by the manufacturing of the channel of 20°. As the angle is narrow, the mill creates, close to the main channel, an area where the width of the secondary channel is much larger than its height. So, there is part of the main flow that is automatically driven into this area (Fig. 8) and this makes easier the aspiration of the continuous phase into the secondary channel.

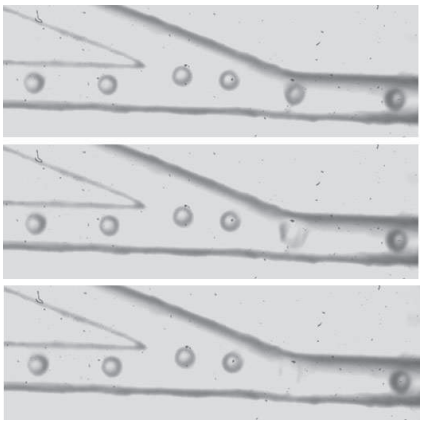

Figure 8. Droplet explosion by contact with a wall in a Y-junction with an angle of 20° when there is no aspiration applied.

Nevertheless, it also brings the droplets closer to the walls even when there is no aspiration flow rate applied. Due to the mechanical stress applied during milling, the roughness of the channels is pretty important and difficult to control. In some cases, the explosion of droplets by contact with the secondary channel walls is observed, and this will automatically interfere with the regularity of the droplet and, consequently, the particles. To prevent this, a T-junction that keeps more droplets at the centre of the channels is used in order to withdraw continuous phase for experiments during the change of solvent around particles.

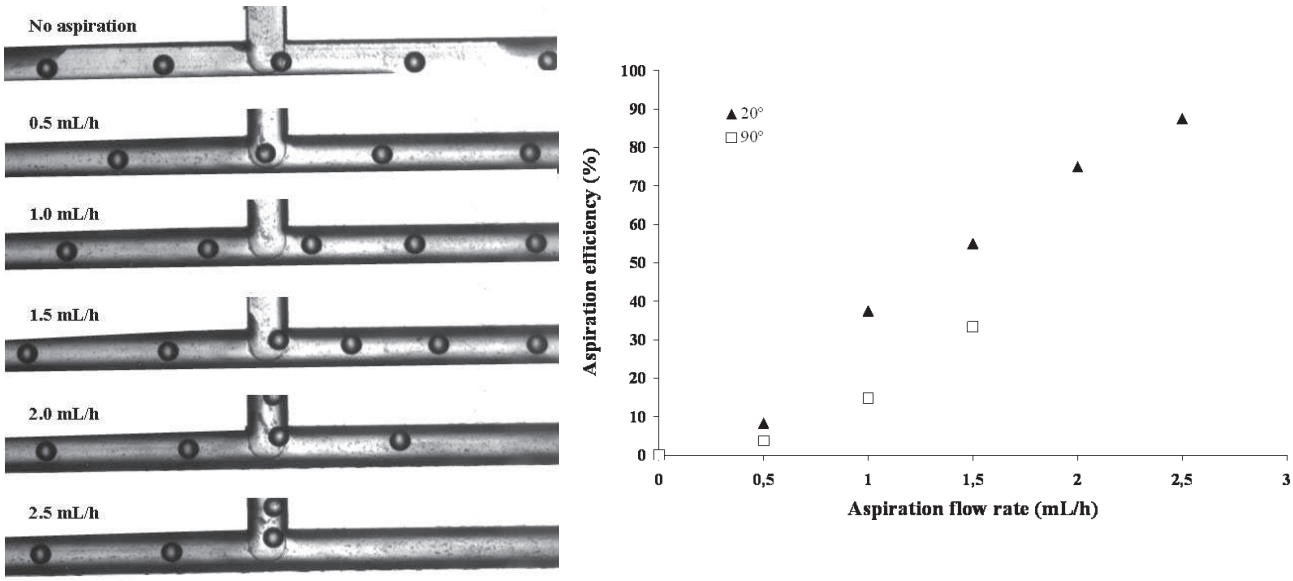

Figure 7. Progressive aspiration of the continuous phase in a T-junction (left), and comparison of the aspiration efficiency between an angle of 20° (▲) and 90° (□).

4.3 Change of Continuous Phase

In order to change the continuous phase around the particles, the injection of a new phase and the withdrawal of the old phase must be coupled. The aim is to find operating conditions where carrier fluid can be easily replaced by a new one. To obtain the change of continuous phase, it is necessary to create a laminar flow between the old and the new one; the new phase must then be injected from one part of the channel and the old one withdrawn from the other part. Considering the limitations on the flow rates of aspiration, more than one secondary channel is necessary to withdraw the old phase. Preliminary tests showed that it was necessary to inject a phase miscible with the aqueous phase carrying the particles. Even if the angle of 20° has proved to create unstable flows, a first experiment is conducted in a device with this type of secondary channels (Fig. 9).

The initial particle flow was generated with an aqueous flow rate of 4 mL h^{-1}. A solution of BTB is used as miscible fluid and the flow rate of injection is fixed at 4 mL h^{-1}. As the initial aqueous phase and the BTB solution have comparable physico-chemical properties and flow is laminar, half of the channel is occupied by BTB and half by the aqueous solution. In this configuration, any change of level in the channel is easily noticeable. The first aspiration site is located at 10 cm from the injection site and the second aspiration site at 20 cm.

A first aspiration is applied; aspiration flow rate is increased up to 2 mL h^{-1}. At this flow rate, the water level has appreciably decreased to a half. Due to wall effects, some BTB is aspired though the withdrawal channel. A second aspiration is then added with the first aspiration set at 2 mL h^{-1}. Aspiration flow rate is again raised up to 2 mL h^{-1}. The main channel is practically full of BTB after the second aspiration, but again some BTB is aspired through the secondary channel. It seems then that the two aspiration channels were necessary to first remove carrier fluid after the injection of the BTB solution. This number may eventually be reduced if carrier fluid is aspired before the injection of BTB and the injection flow rate is increased. In order to reduce diffusion phenomena, withdrawal channels should be placed closer to secondary fluid injection.

A new device is then built with the T-junction as secondary channels in order to keep a regular particle flow. In this device, a third aspiration site is added because a higher aqueous flow rate is used (8 mL h^{-1}) in order to manipulate spherical particles. The aspiration sites are located 5 cm from each other and from the injection in order to reduce the diffusion between both phases. An example of solvent change around particles in this new device is presented in Fig. 10. To better illustrate the

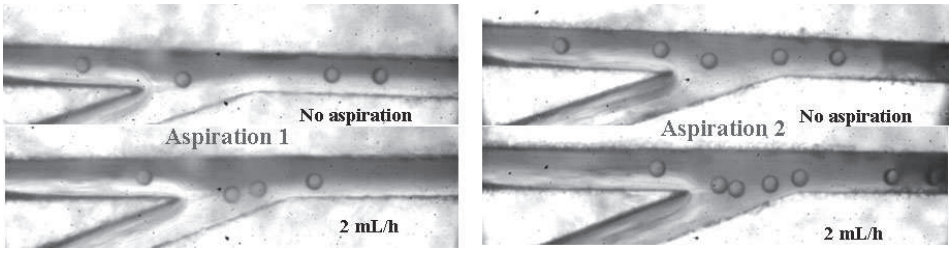

Figure 9. Replacement of the aqueous phase carrying the particles by a BTB solution with two consecutive aspiration channels.

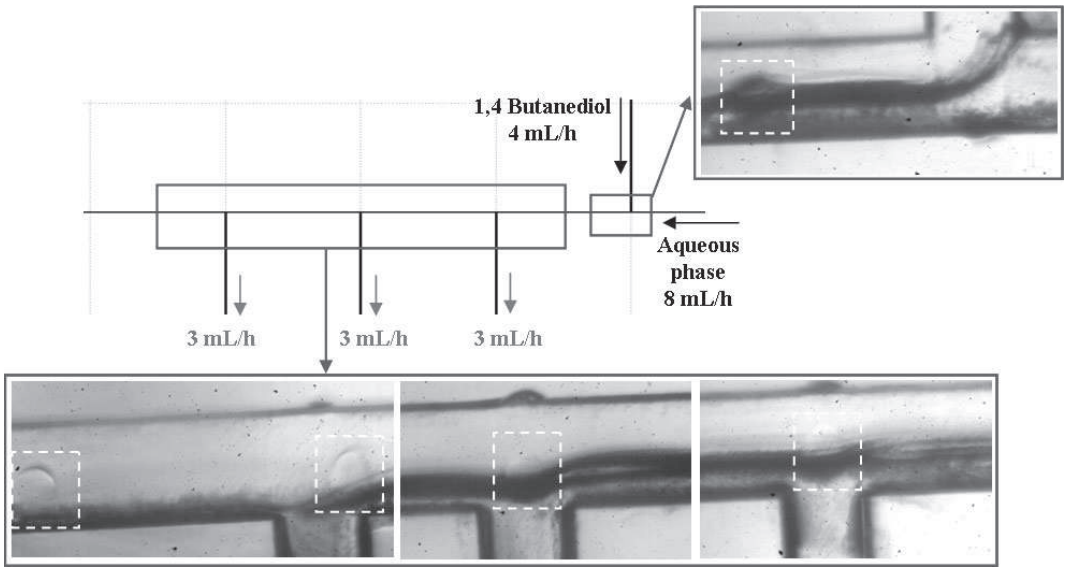

Figure 10. Replacement of the aqueous phase carrying the particles (dotted white squares) by 1,4-butanediol with three consecutive aspiration channels.

transfer of particles from one phase to another, 1,4-butanediol is used because it has a clear interface with water once put in contact in a microchannel.

Before introducing particles, the flow rate of the introduction of 1,4-butanediol is determined with a droplet flow. 1,4-butanediol is indeed far more viscous than the aqueous solution and, thus, it occupies a bigger part of the channel. If the level of 1,4-butanediol is too significant, the droplets and, consequently, particles will enter in contact with the wall at the bottom of the channel. With an equivalent flow rate of aqueous solution and 1,4-butanediol of 8 mL h^{-1}, all the droplets touch the wall and explode. At 6 mL h^{-1}, half of the droplets explode by contact with the wall. Finally, the flow rate of 1,4-butanediol is set at 4 mL h^{-1}, which is the highest flow rate possible without droplet explosion.

When a particle reaches the T-junction, it is first repulsed at the bottom of the channel and close to the wall by the introduction of the new phase. Then, it automatically tries to regain the centre of the channel, troubling the interface (image at the injection site). As long as the particle advances through the channel, it passes from the aqueous phase to the 1,4-butanediol and is located at the interface between both phases at each aspiration site because of the attraction; it creates dragging on the interface (double interface appearing on the image of the second aspiration site). The level of the aqueous phase progressively decreases at each aspiration site until there is one phase left at the last T-junction. The global aspiration flow rate applied is 9 mL h^{-1}, whereas the initial water flow rate was 8 mL h^{-1}. The difference may be the result of mixing effects because of the troubles created at the interface by the particles. As a consequence, the particles are less distant from each other: two particles are visible at the last aspiration site. The particle pattern obtained after the change of solvent is time-proof.

4.4 Particles Encapsulation

In this part, the objective is to trap one particle into a single droplet. As the chain of particles arriving at the injection point is regular, there will only be one flow rate of injection that will correspond to the entrapment of a single particle into one droplet in a stable sequence. In order to add a degree of freedom on the size of the droplet surrounding the particle, an aspiration module is positioned just before the injection of the new phase. The coupling of an aspiration module and the injection module helps regulating the size of the new droplet by acting on the distance between the particles. The modules used in this case are cross-junction so that particles are kept in the middle of the channel during injection or aspiration. In these experiments, octanol is used directly on the aqueous solution carrying particles. Two different initial flow rates of monomer are represented on Fig. 11; aqueous flow rate is imposed at 8 mL h^{-1}.

For each monomer and aspiration flow rate, the octanol flow rate is progressively increased: at low flow rates, one or more particles can be trapped in a single droplet. At high flow rates, the droplets can be generated without particles inside. The graph of Fig. 11 plots the synchronization flow rates gathered during experiments for each operating condition. It is no-

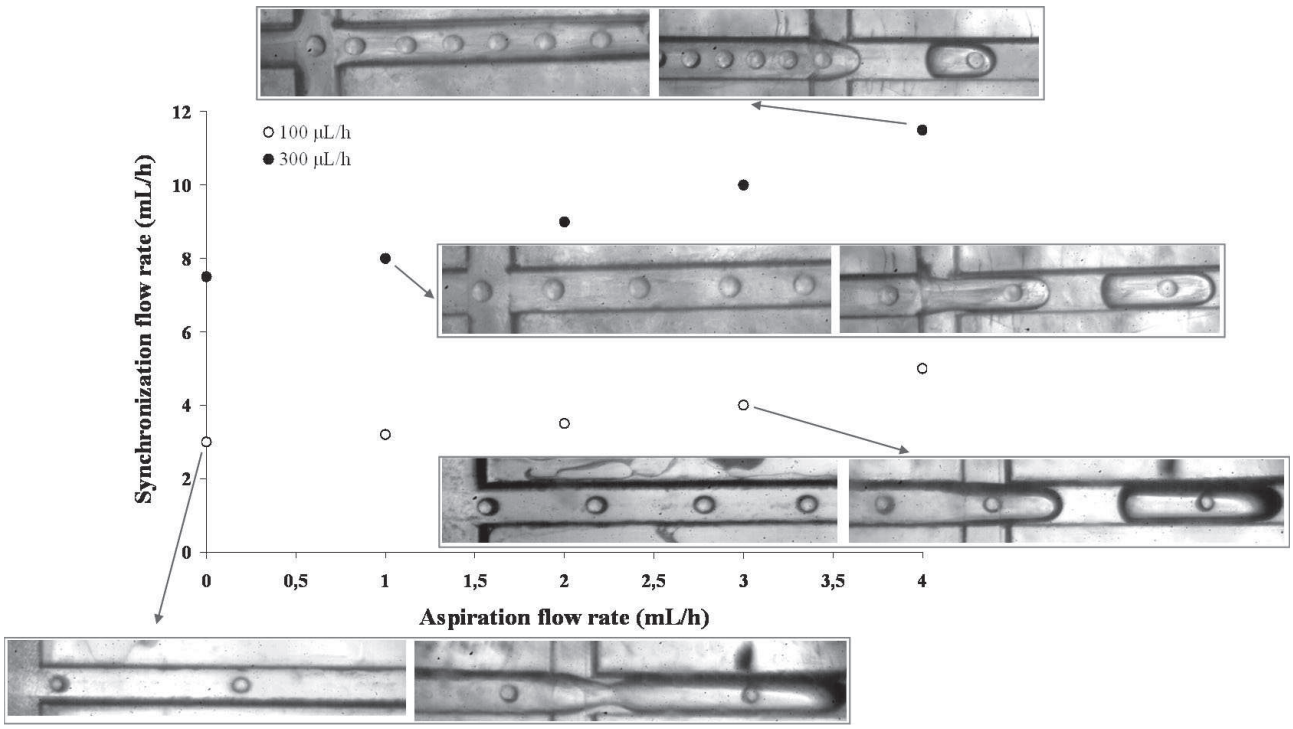

Figure 11. Research of the synchronization flow rate of the third phase function of the aspiration flow rate and the initial flow rate of the monomer.

ticeable that the distance between particles strongly interacts with the synchronization flow rate and, consequently, the frequency and the size of the droplets generated. The droplets generated are the consequence of the physico-chemical properties of the two phases involved and the size of droplets obtained will change if another phase is used but adding the aspiration module can notably reduce its size. If aspiration is too important, it may induce contact between particles or the fall into the bottom of the channel. The aspiration in this case is also subject to limitations not to modify the particle pattern.

5 Conclusion

A complex multioperation microdevice including droplet generation, polymerization part, and particles handling is reported here. Polymer particles generated are monodisperse and in the range of 70–200 microns. This range can easily be widened by changing the inner diameters of capillaries that constitute the device. The feasibility of coupling aspiration and injection modules in order to perform continuous operations, such as solvent change or particles encapsulation in microchannels has been demonstrated. From the results, it is possible to generate complex solid structures. For instance, by coupling solvent change and particles encapsulation, onion-like structures with a chosen nature are reachable. Of course, the specific device of this study presents constraints which limit the operating domain. These constraints are mainly due to the mechanical etching that implies roughness, but this could be solved in second generation devices. The methodology and the analysis of this paper can be applied to design other devices for the generation of other micro-objects.

Acknowledgements

The authors acknowledge the French Ministry of Education and Research for having funded this work through the grant ANR n NT05-1_45715.

The authors have declared no conflict of interest.

Symbols used

d	[m]	diameter of the microchannel
f	[s^{-1}]	drop or particle frequency of generation
f	[s^{-1}]	frequency of generation of the droplet containing particles
$h\upsilon$	[J]	energy brought to the system by radiation
l	[m]	length of the microchannel
L_{ext}	[m]	length of the droplet containing particles
L_g	[m]	drop length
L_i	[m]	length of the interval between droplets
L_p	[m]	particle length
$L_{pattern}$	[m]	length of the pattern
N_{int}	[–]	number of particles included in a droplet
Q_c	[$m^3\ s^{-1}$]	flow rate of the continuous phase
Q_d	[$m^3\ s^{-1}$]	flow rate of the dispersed phase
Q_3	[$m^3\ s^{-1}$]	flow rate of the third phase
R_c	[–]	roughness of the microchannel wall
$T°$	[J]	energy brought to the system by temperature
v	[$m\ s^{-2}$]	drop or particle velocity
v_{ext}	[$m\ s^{-2}$]	velocity of the droplet containing particles
w_{ext}	[m]	width of the droplet containing particles
w_g	[m]	drop width
w_p	[m]	particle width
a	[°]	angle between two channels
θ	[°]	contact angle between the fluid and the microchannel wall
$[\varphi\chi]$	[–]	physico-chemical properties of fluids

References

[1] D. Wilms, J. Klos, H. Frey, *Macromol. Chem. Phys.* **2008**, *209 (4)*, 343.
[2] M. Miyazaki et al., *Micro and Nanosystem* **2009**, *1 (3)*, 193.
[3] C. Serra et al., *Langmuir* **2007**, *23*, 7745.
[4] N. Berton et al., *Chem. Eng. J.* **2008**, *135 (1)*, S93.
[5] S. Sugiura, M. Nakajima, H. Itou, M. Seki, *Macromol. Rapid Commun.* **2001**, *22*, 773.
[6] F. Ikkai, S. Iwamoto, E. Adachi, M. Nakajima, *Colloid Polym. Sci.* **2005**, *283*, 1149.
[7] M. Seo et al., *Langmuir* **2005**, *21*, 11614.
[8] D. Dendukuri, K. Tsoi, T. A. Hatton, P. S. Doyle, *Langmuir* **2005**, *21*, 2113.
[9] J. D. Tice, H. Song, A. D. Lyon, R. F. Ismagilov, *Langmuir* **2003**, *19*, 9127.
[10] Z. Nie et al., *J. Am. Chem. Soc.* **2005**, *127*, 8058.
[11] T. Nisisako, T. Torii, T. Higuchi, *Chem. Eng. J.* **2004**, *101*, 23.
[12] Z. Nie et al., *J. Am. Chem. Soc.* **2006**, *128 (29)*, 9408.
[13] A. Marcati et al., *Chem. Eng. Technol.* **2009**, *32 (11)*, 1823.
[14] L. Prat, F. Sarrazin, J. Tasseli, A. Marty, *Microfluid. Nanofluid.* **2006**, *2 (3)*, 271.